ISSN: 2414-1895 DOI: 10.6919/ICJE.202405_10(5).0032

Deformation Behavior of FeCoCrNiMn High Entropy Alloy Fabricated by Additive Manufacturing under Constant High Strain Rate

Kaige Wang[1, a], Zhuo Chen[2], Xinran Guan[3], Aihan Feng[3], Guojian Cao[4], Da Hua[4], Hao Wang[1, b, *]

[1] Interdisciplinary Centre for Additive Manufacturing (ICAM), School of Materials and Chemistry, University of Shanghai for Science and Technology, Shanghai, 200093, China

[2] Aerospace Haiying (Harbin) Titanium Industry Co., Ltd, Harbin, 150028, China

[3] School of Materials Science and Engineering, Tongji University, Shanghai, 201804, China

[4] Yangtze Delta Region Institute of Advanced Materials, Suzhou, 215100, China

[a]1459240048@qq.com; [b, *] haowang7@usst.edu.cn

Abstract

High Entropy Alloys (HEAs), as a new class of alloy materials, have shown broad application prospects in the field of impact engineering due to their outstanding performance characteristics. However, existing research on their mechanical behavior has primarily focused on quasi-static conditions, with relatively limited studies on HEAs produced by additive manufacturing. This paper systematically investigates the dynamic deformation behavior and microstructural evolution of additive manufactured FeCoNiCrMn high entropy alloys under constant high strain rates. A series of detailed dynamic tensile tests were conducted on the alloy at various constant high strain rates using a high-speed tensile testing machine. The grain morphology was examined using Electron Backscatter Diffraction (EBSD) technology, and the hardening mechanisms related to strain rate were revealed through precise calculation of dislocation density. The study found that the additive manufactured FeCoNiCrMn high entropy alloys exhibited significant strain rate sensitivity under high strain, especially showing considerable mechanical performance improvement at extremely high strain rates, indicating that the alloy has excellent application potential under rapid loading conditions. Furthermore, the analysis of the alloy's fracture surfaces revealed a mix of ductile and brittle fracture features, further confirming the complex stress response mechanism of the material under dynamic loading. These findings not only reveal the behavioral characteristics of additive manufactured FeCoNiCrMn high entropy alloys under dynamic loading conditions but also provide valuable guidance for their application in areas such as high-speed impact and machining.

Keywords

Dynamic Deformation Behavior; High-Speed Tensile Testing; AM-FeCoNiCrMn High Entropy Alloy; Hardening Mechanism.

1. Introduction

Selective Laser Melting (SLM) is a powder bed fusion 3D printing technology that employs a high-energy-density laser beam to scan and melt metal powder layer by layer. SLM technology is capable

ISSN: 2414-1895 DOI: 10.6919/ICJE.202405_10(5).0032

of producing parts with virtually no manufacturing constraints, making it especially suitable for manufacturing complex geometric shapes or parts that are difficult to produce with traditional manufacturing methods. This technology allows for precise control over the melting process, thereby producing parts with high density and excellent mechanical properties. Consequently, additive manufacturing (AM) products find extensive applications in fields such as aerospace and defense industries. In these sectors, AM product components often face impacts from dynamic loads; for example, rockets and spacecraft experience extreme vibrations and shock forces during launch; operational satellites and other spacecraft might encounter high-speed impacts from space debris or micro-meteoroids; and collisions with birds during landing, among others. Among them, Multi-Principal Element High Entropy Alloys (HEAs) processed through SLM are one of the most common alloys and are considered some of the most important engineering materials in the aviation industry to date[1-5].

High Entropy Alloys (HEAs) belong to a very unique category of alloys characterized by their high mixing entropy and approximately equiatomic ratios of constituent atoms. They form a solid solution with a disordered arrangement of multiple principal elements within a simple lattice structure. This structure endows HEAs with several notable properties, such as high strength, good ductility at low temperatures, and a high resistance to hydrogen embrittlement[6-11]. The FeCoCrNiMn alloy is a typical representative of High Entropy Alloys (HEAs) and has been confirmed as a single-phase Face-Centered Cubic (FCC) solid solution. Its unique chemical composition and microstructure contribute to its excellent mechanical strength, corrosion resistance, and stable performance under extreme conditions. These characteristics have opened up broad applications in numerous industries, including aerospace, automotive, biomedical, energy, and protective equipment. Particularly, its exceptional combination of strength and toughness, along with its capabilities for high-temperature and corrosion resistance, make it an ideal material choice for critical components in complex application environments.[12-18].These characteristics endow the FeCoCrNiMn alloy with a wide range of practical prospects, particularly in facing dynamic impact applications in aerospace and defense engineering.

Consequently, for Additive Manufacturing (AM) product components, impact resistance has become a key performance indicator..Research has shown that the load-bearing capacity of specific materials can be divided into three intervals based on the strain rate: static ($<10^{-5}$ s^{-1}), quasi-static (10^{-5} to 10^{-1} s^{-1}), and dynamic ($>10^{-1}$ s^{-1}). Under static loads, the impact of strain rate on material performance is almost negligible. However, when the strain rate exceeds 10^{-1} s^{-1}, its influence becomes significant, and the material's response under dynamic loading differs greatly from its behavior under static or quasi-static conditions. To date, several studies have been conducted on the dynamic performance of single-phase Face-Centered Cubic (FCC) CoCrFeNi-based High Entropy Alloys (HEAs).[19-22].

Kumar et al. first unveiled the compressive deformation characteristics of Al0.1CrFeCoNi high-entropy alloy under high strain rates, revealing its high strain rate sensitivity and significant strain hardening effect, accompanied by the formation of a large amount of twinning. [23].Li et al. discovered a pronounced resistance of the $Al_{0.3}$CoCrFeNi high-entropy alloy (HEA) to shear localization during dynamic loading of hat-shaped specimens. [24].Researchers Foley et al. observed the occurrence of deformation twinning and microbands in CoCrFeMnNi high-entropy alloy when the strain rate reached $8000s^{-1}$ [25].These research findings indicate significant potential for these HEAs in impact engineering. However, traditionally, the study of dynamic mechanical properties relies on Hopkinson bar experiments, which have significant limitations, particularly in experimental setup, specimen size, and shape.These factors may lead to discontinuity and inconsistency in strain rates during the experimental process, thereby affecting the accuracy and reliability of experimental results. In comparison, high-speed tensile testing machines, by finely adjusting experimental parameters, can maintain relatively constant or controllable strain rates throughout the experiment, thus achieving precise control over strain rates.This characteristic is crucial for gaining a deeper understanding of material behavior at specific strain rates, especially for materials with significant sensitivity to strain rate. The ability to control strain rates is therefore paramount in such cases,

ISSN: 2414-1895 DOI: 10.6919/ICJE.202405_10(5).0032

facilitating precise investigations into material responses under varying dynamic loading conditions.Nevertheless, revealing the changes in alloy microstructures under dynamic strain rate conditions and their complex relationship with macroscopic mechanical properties remains a significant challenge. This necessitates the adoption of more refined experimental techniques and analytical methods to ensure accurate capturing of the intrinsic connections between material behavior and microstructural evolution. [26-28].

In this study, we conducted dynamic mechanical analysis on a single-phase FCC structured AM-FeCoCrNiMnHEA. By integrating high-speed tensile testing equipment and high-speed photography techniques, dynamic tensile tests were performed on this high-entropy alloy. Through the analysis of microstructures at different scales, fracture modes were explored. Additionally, electron backscatter diffraction (EBSD) was utilized to study grain morphology and calculate dislocation density, elucidating the hardening mechanisms associated with strain rate.

2. Materials and Methods

2.1 Materials Preparation

In this study, we utilized atomically balanced FeCoCrNiMn alloy powder to ensure homogeneity and flowability, suitable for the Selective Laser Melting (SLM) process. Carbon steel was chosen as the printing substrate to provide adequate mechanical support and thermal conductivity. An in-house developed SLM printer (DiMetal-100 H) was selected, offering control over laser power, scanning speed, scan spacing, and layer thickness.The following process parameters were employed to prepare the tensile specimens for this experiment: a substrate preheating temperature of 150°C was applied to minimize thermal stresses and deformation of the specimens during printing; The laser power was set to 300W to ensure sufficient energy density for powder melting; The scanning speed was set to 900mm/s to balance printing speed with the stability of the molten pool;The scanning spacing was adjusted to 100μm to ensure good coverage and molding quality;The layer thickness was set to 30μm to achieve better layering accuracy and surface smoothness.

2.2 Experimental Procedure

All experiments were conducted on a high-speed tensile testing machine, encompassing axial tensile tests at four different strain rates (1, 10, 100, 1000s^{-1}), covering a range from 1s^{-1} to 1000s^{-1} in strain rates. At low strain rates of 1 and 10s^{-1}, load data were directly obtained from the piezoelectric force sensor of the testing equipment. However, at high strain rates of 100 and 1000s^{-1}, to minimize measurement noise and system vibration, strain gauges were affixed to the specimens.Strain data during the experiments were acquired using Digital Image Correlation (DIC) technique. This involved applying speckle patterns on the surface of the specimens, recording the experimental process using high-speed cameras, and analyzing the deformation of the specimens using VIC-2D software. After appropriate processing of the raw signals from the experiments, engineering stress-strain curves of the materials were obtained.

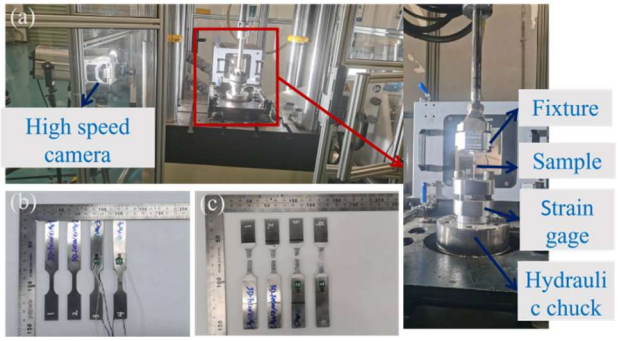

Figure 1. High speed tensile testing system(a);AM-FeCoCrNiMn alloy samples before and after tensile fracture(b,c)

ISSN: 2414-1895 DOI: 10.6919/ICJE.202405_10(5).0032

2.3 Microstructural Characterization

After testing,samples were cut according to standard procedures for metallographic examination. The surfaces of the cut and polished samples were etched for 40 seconds using a solution containing HF (2ml),HNO_3(4ml),and H_2O(50ml)to reveal the microstructure at the fracture surface.The microstructure, phases, and fracture surfaces of the samples were observed using optical microscopy (Keyence VHX-600) and scanning electron microscopy (Hitachi SU5000).Microstructural analysis of the samples after impact was conducted using Electron Backscatter Diffraction(EBSD) in the German Bruker QUANTAX CrystAlign 400i scanning electron microscope. The detection area was located at the fracture surface of the samples.

3. Results and Discussion

3.1 Stress-Strain Relationship

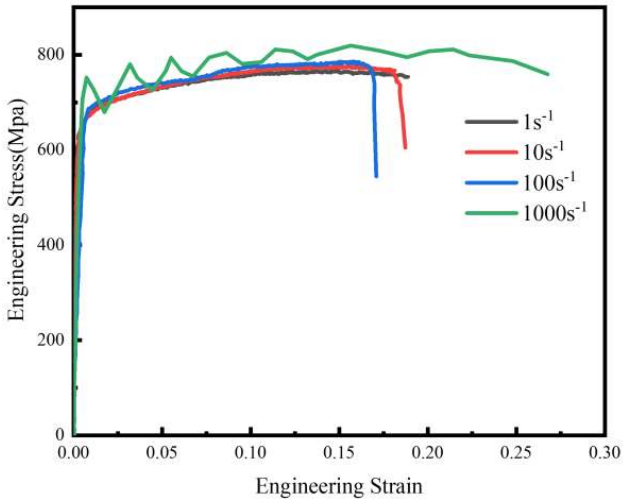

Figure 2. Engineering stress-strain curves of AM-FeCoCrNiMn HEA at different strain rates

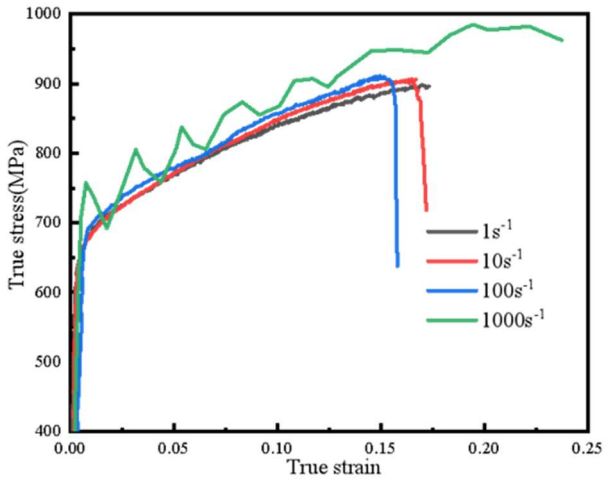

Figure 3. True stress-strain curves of AM-FeCoCrNiMn HEA at different strain rates

ISSN: 2414-1895 DOI: 10.6919/ICJE.202405_10(5).0032

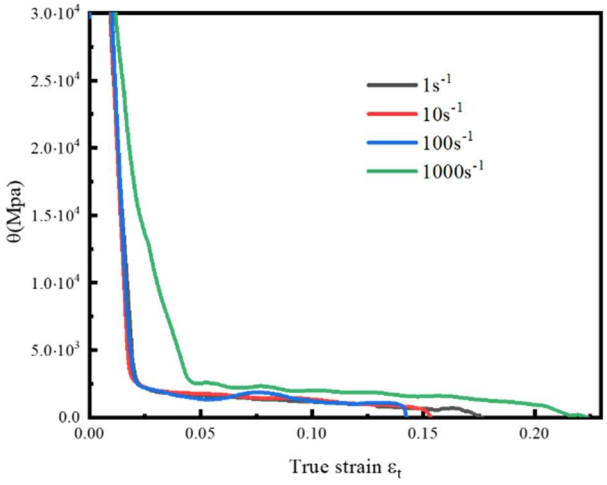

Figure 4. Work hardening rate curves of AM-FeCoCrNiMn HEA at different strain rates

In this study, dynamic tensile experiments were conducted covering four different strain rates: 1, 10, 100, and 1000s^{-1}, encompassing the full range from 1s^{-1} to 1000s^{-1}. Under these experimental conditions, the yield strengths of the FeCoCrNiMn alloy subjected to tensile loading at strain rates of 1 to 1000s^{-1} were measured as 643.8, 647.36, 666.72, and 730.88 MPa, respectively. Correspondingly, the true ultimate tensile stresses were determined as 897.93, 906.88, 911.19, and 985.21 MPa, while the total strains were recorded as 0.17, 0.17, 0.16, and 0.24, respectively.By comparing the tensile test results under different strain rates, it is evident that the FeCoCrNiMn high-entropy alloy exhibits significant strain hardening effects at higher strain rates. Moreover, the strain rate has a notable influence on the material's deformation behavior, which is typically manifested in the material's plastic deformation capacity and the ultimate strain it can withstand before fracture.The experimental data indicates that varying the strain rate results in significantly different ultimate strains exhibited by the samples. Under low strain rate conditions (such as 1s^{-1} to 10s^{-1}), the material has sufficient time for microstructural adjustments such as dislocation movement and crystal slip, promoting plastic deformation, and consequently achieving higher ultimate strain values.The slight fluctuations observed near the fracture point in the curves under low strain rates can be attributed to localized instability phenomena. At this stage, the material exhibits more pronounced deformation as it withstands increased stress, leading to fluctuations in the stress-strain curve.As the strain rate increases, such as at 100s^{-1}, the deformation rate of the material accelerates, leading to a shorter available time for microstructural adjustments. Consequently, the plastic deformation capacity decreases, resulting in a reduction in the ultimate strain.At extremely high strain rates, such as 1000s^{-1}, rapid material deformation leads to the accumulation of localized heat, while the heat cannot dissipate quickly enough through thermal conduction. This results in a sharp increase in local temperature.This phenomenon triggers thermal softening effects, significantly reducing the material's flow stress. This allows the material to exhibit greater plastic deformation before fracture occurs.Additionally, as indicated by the experimental results, additive manufacturing of FeCoCrNiMn high-entropy alloy enhances both strength and ductility under high strain rate conditions. This finding suggests a significant sensitivity of additive manufacturing FeCoCrNiMn high-entropy alloy to strain rate, with mechanical properties being optimized with increasing strain rates.This sensitivity reflects the material's internal structure's ability to respond to changes in deformation rate, which may involve complex mechanisms such as dislocation motion, twinning, phase transformation, and more. The increase in plasticity under high strain rates suggests that the material may activate additional plastic deformation pathways, such as dislocation slip mechanisms. These pathways aid in absorbing more deformation energy, thereby enhancing ductility. The

ISSN: 2414-1895 DOI: 10.6919/ICJE.202405_10(5).0032

simultaneous enhancement of strength and ductility in AM-FeCoCrNiMn high-entropy alloy under high strain rates further demonstrates its capability to maintain microstructural stability under extreme conditions. This is particularly crucial for applications that demand high performance from materials under extreme conditions such as high-speed impact and machining.

3.2 Dynamic Deformation and Fracture Behavior

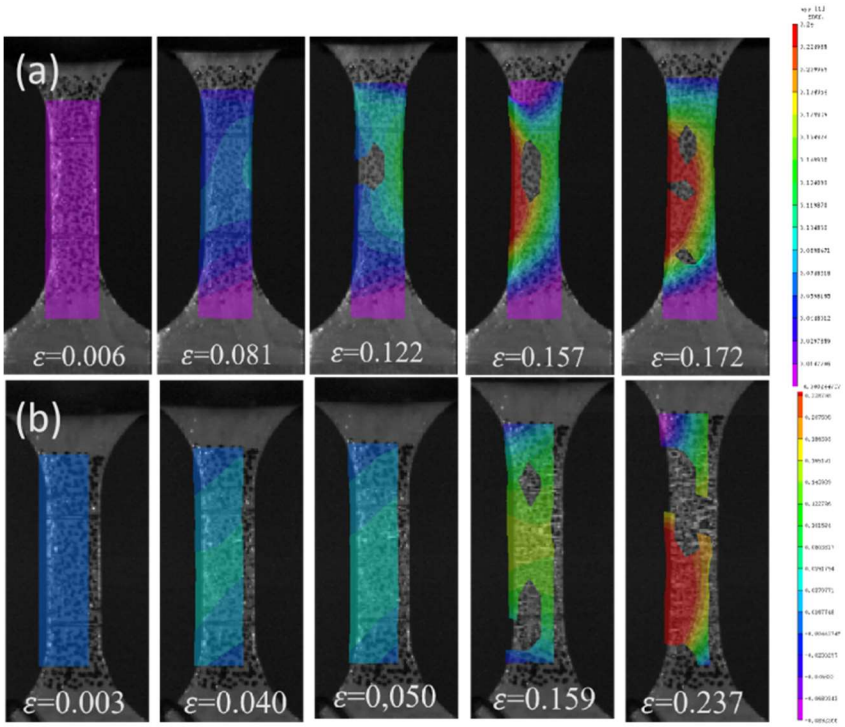

Figure 5. Strain distribution of samples at different times during high-speed tensile testing.(a)1s^{-1},(b)1000s^{-1}

As shown in Figure 5, real-time recording of dynamic tensile tests was conducted using high-speed photography, combined with Digital Image Correlation (DIC) analysis technique to assess stress fields. This enabled accurate tracking of the deformation behavior of the samples during the loading process.In the experiment, the sample surfaces were coated with speckle patterns for DIC analysis. This allowed for the visualization of stress distribution changes through color variations, providing a clear and intuitive representation of the evolving stress fields.The unidentified portions in the image are due to sample vibrations during the tensile process, causing the speckle patterns to be unrecognized. However, this does not affect the overall variation of the stress field.In the initial loading stages, the speckle pattern appears blue, indicating relatively low stress levels. As the experiment progresses, yellow areas begin to appear in the middle section of the sample. The appearance of yellow areas signifies the onset of stress concentration, which typically occurs when the material approaches or reaches its yield strength. This formation and expansion of yellow areas can be interpreted as the initiation of material yielding. As deformation progresses, the expansion of red areas resulting from stress concentration reflects the material's hardening behavior. The eventual formation and expansion of red areas herald the imminent fracture of the material.Before reaching fracture, the material experiences the greatest stress concentration and localized deformation in these areas, which are typically the locations of future fracture surfaces.

Figure 6 shows the tensile fracture morphology under different strain rates. Macroscopically, the fracture surfaces do not exhibit obvious necking phenomena. However, upon closer examination with local magnification, numerous voids can be observed, primarily due to gaps or uneven coverage during material deposition.However, considering that the printed material maintains a relatively high elongation, it is inferred that the number of voids is likely small and their sizes are small as well, with

ISSN: 2414-1895 DOI: 10.6919/ICJE.202405_10(5).0032

negligible impact on conventional mechanical properties. However, related studies suggest that dispersed voids can significantly affect fatigue performance. Additionally, the fracture surface exhibits a "ductile-brittle" mixed fracture characteristic overall, with noticeable cleavage surfaces and transgranular fracture phenomena.In the transgranular fracture grains, distinct slip traces were observed. However, differences were noted among samples subjected to strain rates of 1000 s^{-1} (as shown in (c, f, j, l)), where single slip was predominant, while samples subjected to strain rates of 1 s^{-1}, 10 s^{-1}, and 100 s^{-1} exhibited multiple slips as the main feature. The initiation of multiple slips promotes dislocation interactions within the grain, leading to the accumulation, crossing, and recombination of dislocations, thereby affecting the material's plastic deformation capacity.From the tensile curves, it can also be observed that the sample subjected to a strain rate of 1000 s^{-1} exhibits a higher elongation.

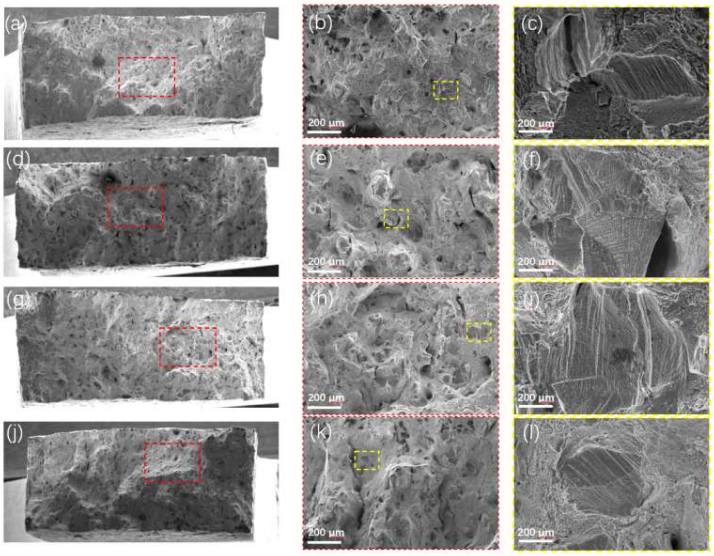

Figure 6. Test the fracture surface of the sample at different strain rates.(a,b,c)1s^{-1},(d,e,f)10s^{-1},(g,h,i)100s^{-1},(j,k,l)1000s^{-1}

3.3 Microstructural Evolution

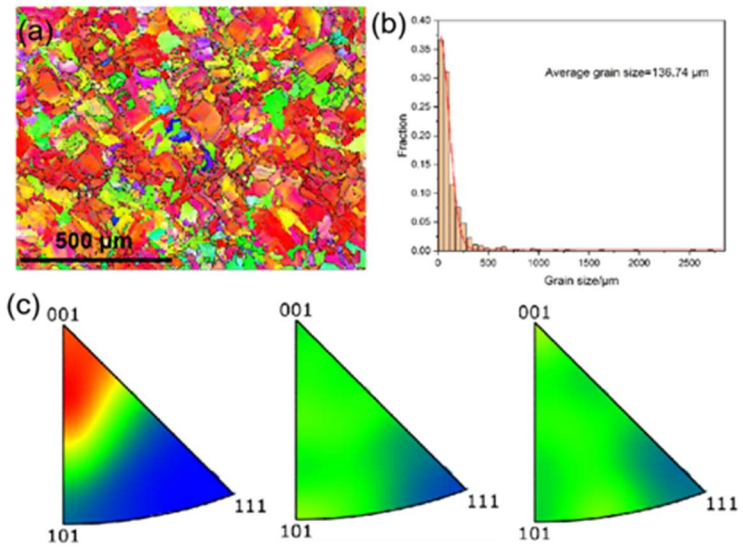

Figure 7. Microscopic analysis of undeformed original group samples using EBSD:(a)Grain distribution,(b)grain size,(c)IPF

ISSN: 2414-1895 DOI: 10.6919/ICJE.202405_10(5).0032

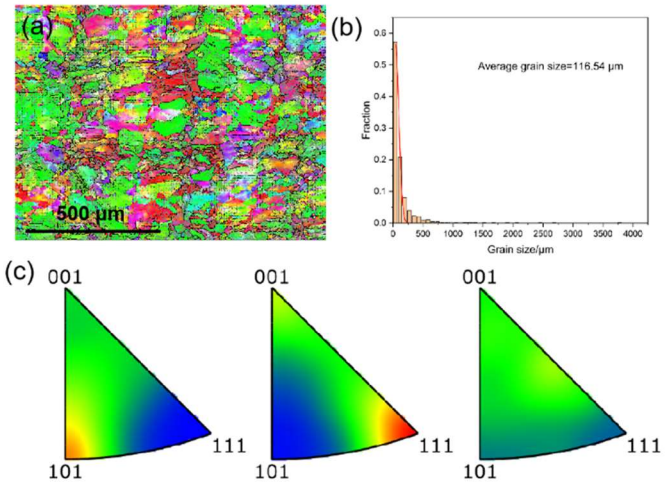

Figure 8. Analysis of the microstructure of samples at a strain rate of 1000s^{-1} using EBSD:(a)Grain distribution,(b)grain size,(c)IPF

Figures 7 and 8 present the microstructural evolution near the fracture surface of the FeCoNiCrMn alloy after high-speed tensile testing. Considering the significant strain concentration near the fracture surface, this could severely impact the identification accuracy of Electron Backscatter Diffraction (EBSD). Therefore, in this study, the EBSD characterization position was located approximately 2mm away from the fracture surface.Through the inverse pole figure (IPF) maps, it is evident that there exists a preferred orientation of {001}//ND axis in the initial microstructure, which may be related to recrystallized grains formed during additive manufacturing. To accommodate significant strains, grains undergo an orientation rotation from {001}//ND axis to {111}//TD axis under the action of maximum shear stress. For FCC metals, {111}<110> is the predominant slip system.Therefore, during uniaxial tensile deformation, grains undergo crystal rotation, aligning the direction of the slip system with the direction of maximum shear stress. This promotes a preferred orientation of {111} planes along the TD axis, enabling the grains to efficiently accommodate external strains.Furthermore, under high-speed deformation, there is a significant refinement in grain size in the fracture region, with the proportion of small grains (~10μm) increasing from 37% to 57%. However, no obvious adiabatic shear bands were observed in the fracture microstructure. Instead, within the grain interiors, some discontinuous black regions with large-angle grain boundaries were notably observed in Figure 7(a), which is a typical characteristic of continuous dynamic recrystallization mechanism.Therefore, we speculate that the grain refinement mechanism is due to the rapid increase in dislocation density within the material under high-speed deformation. As dislocations move, they become entangled with each other, forming dislocation walls or subgrain boundaries. These subgrain boundaries, which initially exhibit characteristics of low-angle grain boundaries, gradually transform into high-angle grain boundaries as they locally absorb dislocations. Consequently, this process leads to the formation of a discontinuous structure comprising both low-angle and high-angle grain boundaries.

To verify this conclusion, we performed calculations based on the dislocation density tensor theory to quantify the geometrically necessary dislocation distribution (GND). By quantifying the GND density and plotting its distribution, we can visually represent the distribution of strain gradients within different grains. This approach aids in studying the micro mechanisms of plastic deformation. The average GND densities for the original microstructure and the microstructure near the fracture surface were determined to be 6.1965×1013 m^{-2} and 7.7508×1014 $m^{-2,}$ respectively.It can be observed that the dislocation density near the fracture surface significantly increases, with GND distributed abundantly within the interior of the deformed grains in the form of intragranular substructures.Interestingly, as shown in Figure 8(b), it is more visually apparent through the GND

ISSN: 2414-1895 DOI: 10.6919/ICJE.202405_10(5).0032

distribution near the fracture surface that strain-free grains nucleate at the triple grain boundaries, which may be related to the material's dislocation accumulation mechanism. Furthermore, Figures 8(a, b) depict local line scans of GND density along the residual deformation structures, demonstrating that substructures under different deformation levels exhibit distinct orientation characteristics.For the original samples, GND exhibits a long-range ordered and uniform distribution, with a relatively low dislocation density of approximately 9.8×1013 m^{-2}.In contrast, for the samples near the fracture surface, the overall GND density increases, but still maintains a long-range ordered distribution. However, there are noticeable peaks in certain regions, indicating that dislocation motion on densely packed planes is impeded, leading to the local entanglement of dislocations.Additionally, it is observed that the GND density at grain boundaries is significantly higher than that in the grain interior. FCC-structured materials possess multiple slip systems, implying that they can readily undergo plastic deformation on various slip planes and directions. Therefore, the increase in strain effectively promotes the formation of dislocations and the accumulation of GNDs at grain boundaries.

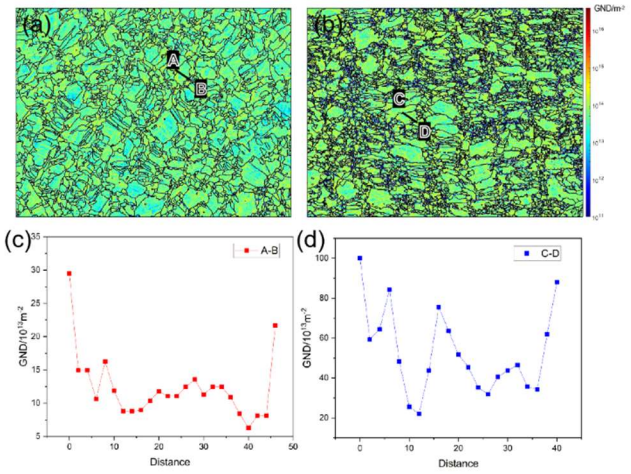

Figure 9. GND distribution maps of samples in different states:(a,c)undeformed tissue,(b,d)strain rate of 1000s^{-1}

4. Conclusion

This study employed high-speed photography technology in conjunction with a high-speed tensile testing apparatus to conduct dynamic mechanical performance analysis on the single-phase FCC-structured AM-FeCoCrNiMn high-entropy alloy.By analyzing its microstructural characteristics at different scales, this study investigated the fracture behavior of the alloy. Additionally, Electron Backscatter Diffraction (EBSD) technique was employed to observe grain structures and calculate dislocation densities, thereby revealing the strain-rate-dependent hardening behavior of the alloy. The following conclusions were drawn:

(1) Under high-speed tensile conditions, the fracture surface of the alloy exhibits a mixed "ductile-brittle" fracture behavior overall, accompanied by pronounced dimples, cleavage facets, and transgranular fracture phenomena.

(2) The AM-FeCoCrNiMn high-entropy alloy exhibits sensitivity to strain rate, with its yield strength and ultimate tensile strength increasing with increasing strain rate. Particularly noteworthy is the optimal mechanical performance observed at the extremely high strain rate of 1000s^{-1}. This indicates that the alloy demonstrates excellent mechanical properties under rapid loading conditions, highlighting its potential in applications such as high-speed impact and machining.

(3) The experimental data reveal a significant strengthening of the strain rate-dependent work hardening effect in the AM-FeCoCrNiMn high-entropy alloy. This reflects the enhanced capability of the material to resist further deformation during plastic deformation processes. Such phenomenon suggests that under extreme conditions, the FeCoCrNiMn high-entropy alloy can absorb more

ISSN: 2414-1895 DOI: 10.6919/ICJE.202405_10(5).0032

deformation energy by activating additional plastic deformation mechanisms, thereby enhancing its ductility while maintaining the stability of its microstructure. This is crucial for high-performance applications.

References

[1] Liu, Y.; Meng, J.; Zhu, L.; Chen, H.; Li, Z.; Li, S.; Wang, D.; Wang, Y.; Kosiba, K., Dynamic compressive properties and underlying failure mechanisms of selective laser melted Ti-6Al-4V alloy under high temperature and strain rate conditions. Additive Manufacturing 2022, 54.

[2] Qiao, Y.; Chen, Y.; Cao, F.-H.; Wang, H.-Y.; Dai, L.-H., Dynamic behavior of CrMnFeCoNi high-entropy alloy in impact tension. International Journal of Impact Engineering 2021, 158.

[3] Yao, D.; Wang, J.; An, X.; Zhang, H.; Fu, H.; Yang, X.; Zou, Q., The essential role of initial powder bed state in selective laser melting of 316 L stainless steel. International Journal of Heat and Mass Transfer 2023, 215.

[4] Zhou, C.; Zhou, L.; Li, M.; Tong, Y.; Zhou, Z., Microstructure and mechanical properties of multi-principal component CoCrNiMo medium entropy alloys. Materials Today Communications 2024, 38.

[5] Meng, Z. C.; Wang, K. G.; Ali, T.; Li, D.; Bai, C. G.; Xu, D. S.; Li, S. J.; Feng, A. H.; Gao, G. J.; Yao, J. H.; Fan, Q. B.; Wang, H., Atomistic Investigation of Shock-Induced Amorphization within Micro-Shear Bands in Hexagonal Close-Packed. Acta Metallurgica Sinica -2023-0284.R2.

[6] Cheng, H.; Luo, H.; Pan, Z.; Wang, X.; Zhao, Q.; Fu, Y.; Li, X., Effects of laser powder bed fusion process parameters on microstructure and hydrogen embrittlement of high-entropy alloy. Journal of Materials Science & Technology 2023, 155, 211-226.

[7] Guan, X. R.; Chen, Q.; Qu, S. J.; Cao, G. J.; Wang, H.; Feng, A. H.; Chen, D. L., Adiabatic shear instability in a titanium alloy: Extreme deformation-induced phase transformation, nanotwinning, and grain refinement. Journal of Materials Science & Technology 2023, 150, 104-113.

[8] Guan, X. R.; Chen, Q.; Qu, S. J.; Cao, G. J.; Wang, H.; Ran, X. D.; Feng, A. H.; Chen, D. L., High-strain-rate deformation: Stress-induced phase transformation and nanostructures in a titanium alloy. International Journal of Plasticity 2023, 169.

[9] Meng, Z. C.; Yang, M. M.; Feng, A. H.; Qu, S. J.; Zhao, F.; Yang, L.; Yao, J. H.; Yang, Y.; Fan, Q. B.; Wang, H., Transfer or blockage: Unraveling the interaction between deformation twinning and grain boundary in tantalum under shock loading with molecular dynamics. Journal of Materials Science & Technology 2023, 156, 118-128.

[10] Yang, Y.; Xu, D.; Cao, S.; Wu, S.; Zhu, Z.; Wang, H.; Li, L.; Xin, S.; Qu, L.; Huang, A., Effect of strain rate and temperature on the deformation behavior in a Ti-23.1Nb-2.0Zr-1.0O titanium alloy. Journal of Materials Science & Technology 2021, 73, 52-60.

[11] Zheng, Z.; Chen, Q.; Peng, X.; Wang, H.; Qu, S.; Feng, A.; Xu, T.; Wang, K., Prediction of mechanical properties of AlTiCrVNb high entropy alloys with B2 ordered structure. Journal of Materials Research and Technology 2023, 24, 440-448.

[12] Fu, Y.; Li, J.; Luo, H.; Du, C.; Li, X., Recent advances on environmental corrosion behavior and mechanism of high-entropy alloys. Journal of Materials Science & Technology 2021, 80, 217-233.

[13] George, E. P.; Curtin, W. A.; Tasan, C. C., High entropy alloys: A focused review of mechanical properties and deformation mechanisms. Acta Materialia 2020, 188, 435-474.

[14] Guo, Y.; Liu, R.; Ran, C.; Arab, A.; Geng, H.; Gao, M.; Guo, B.; Zhou, Q.; Zhou, Q.; Chen, P., Ignition and energy release characteristics of energetic high-entropy alloy HfZrTiTa0.2Al0.8 under dynamic loading. Journal of Materials Research and Technology 2024, 28, 2819-2830.

[15] Kumar, A.; Singh, A.; Suhane, A., Mechanically alloyed high entropy alloys: existing challenges and opportunities. Journal of Materials Research and Technology 2022, 17, 2431-2456.

[16] Li, W.; Xie, D.; Li, D.; Zhang, Y.; Gao, Y.; Liaw, P. K., Mechanical behavior of high-entropy alloys. Progress in Materials Science 2021, 118.

[17] Sathiyamoorthi, P.; Kim, H. S., High-entropy alloys with heterogeneous microstructure: Processing and mechanical properties. Progress in Materials Science 2022, 123.

ISSN: 2414-1895 DOI: 10.6919/ICJE.202405_10(5).0032

[18] Sonkusare, R.; Jain, R.; Biswas, K.; Parameswaran, V.; Gurao, N. P., High strain rate compression behaviour of single phase CoCuFeMnNi high entropy alloy. Journal of Alloys and Compounds 2020, 823.

[19] Li, Q. M.; Lu, Y. B.; Meng, H., Further investigation on the dynamic compressive strength enhancement of concrete-like materials based on split Hopkinson pressure bar tests. Part II: Numerical simulations. International Journal of Impact Engineering 2009, 36 (12), 1335-1345.

[20] [20] Tang, Y.; Wang, R.; Xiao, B.; Zhang, Z.; Li, S.; Qiao, J.; Bai, S.; Zhang, Y.; Liaw, P. K., A review on the dynamic-mechanical behaviors of high-entropy alloys. Progress in Materials Science 2023, 135.

[21] Wang, R.; Zhang, H.; Tang, L.; Shao, J.; Xiao, Z.; Chen, Z.; Liu, C.; Tang, J., Adiabatic shear deformation behaviors of cold-rolled copper under different impact loading directions. Materials Science and Engineering: A 2019, 754, 330-338.

[22] You, Z. Y.; Tang, Z. Y.; Wang, B.; Zhang, H. W.; Li, P.; Zhao, L.; Chu, F. B.; Ding, H., Microstructural evolution and deformation behavior of an interstitial TRIP high-entropy alloy under dynamic loading. Materials Science and Engineering: A 2024, 891.

[23] Kumar, N.; Ying, Q.; Nie, X.; Mishra, R. S.; Tang, Z.; Liaw, P. K.; Brennan, R. E.; Doherty, K. J.; Cho, K. C., High strain-rate compressive deformation behavior of the Al0.1CrFeCoNi high entropy alloy. Materials & Design 2015, 86, 598-602.

[24] Li, Z.; Zhao, S.; Diao, H.; Liaw, P. K.; Meyers, M. A., High-velocity deformation of Al(0.3)CoCrFeNi high-entropy alloy: Remarkable resistance to shear failure. Sci Rep 2017, 7, 42742.

[25] Foley, D. L.; Huang, S. H.; Anber, E.; Shanahan, L.; Shen, Y.; Lang, A. C.; Barr, C. M.; Spearot, D.; Lamberson, L.; Taheri, M. L., Simultaneous twinning and microband formation under dynamic compression in a high entropy alloy with a complex energetic landscape. Acta Materialia 2020, 200, 1-11.

[26] Huang, A.; Fensin, S. J.; Meyers, M. A., Strain-rate effects and dynamic behavior of high entropy alloys. Journal of Materials Research and Technology 2023, 22, 307-347.

[27] Ma, E., Unusual dislocation behavior in high-entropy alloys. Scripta Materialia 2020, 181, 127-133.

[28] Nguyen, N. T.; Asghari-Rad, P.; Sathiyamoorthi, P.; Zargaran, A.; Lee, C. S.; Kim, H. S., Publisher Correction: Ultrahigh high-strain-rate superplasticity in a nanostructured high-entropy alloy. Nat Commun 2022, 13 (1), 740.